

# Comparison of MM5 Integrated Water Vapor With Microwave Radiometer, GPS, and Radiosonde Measurements

Adelaide Memmo, Ermanno Fionda, Tiziana Paolucci, Domenico Cimini, *Member, IEEE*, Rossella Ferretti, Stefania Bonafoni, and Piero Ciotti, *Member, IEEE*

**Abstract**—A large dataset of concurrent integrated precipitable water vapor (IPWV) estimates from ground-based microwave radiometers (MWRs), global positioning system (GPS) ground-receivers, and radiosonde observations (RAOBs) has been collected in five different sites in Central Italy. Both MWRs and GPS have shown a capability of accurate and continuous water vapor monitoring. These data are used to study the seasonal and spatial variability of IPWV. A comparison of these data with the IPWV field produced operationally by the nonhydrostatic Mesoscale Model (MM5), running at the University of L'Aquila/Center of Excellence (CETEMPS) is performed in order to find either model shortcomings and to corroborate the IPWV behavior highlighted by the measurements. Both measurements and model outputs span over a period of about one year allowing for a systematic statistical analysis for all the examined stations. The statistical analysis shows a good agreement between GPS and MWR data, whereas discrepancies are found between RAOBs and the other techniques. The IPWV shows the largest diurnal variability, approximately 3%, during the summer season. An overall good agreement is found between the forecasted and observed IPWV. The related statistical parameters show a very low bias (0.001 cm) with a good correlation coefficient (0.939). On the other hands, the seasonal analyses highlight a few discrepancies, mostly due to the MM5 difficulties in correctly forecasting the diurnal cycle.

**Index Terms**—Global positioning system (GPS), Mesoscale Model (MM5), microwave radiometer, water vapor.

## I. INTRODUCTION

**W**ATER vapor is a key parameter in many human technological applications, in the water budget, and in monitoring of greenhouse gases. Accurate observations of water vapor amount, as well as spatial and temporal fluctuations, are important for many reasons, including that water

vapor is one of major error sources in radio astronomical interferometry, radio wave propagation, and geodesy applications.

A large amount of data derived by numerical weather prediction model output can be validated either using *in situ* measurements (as temperature, relative humidity, pressure, etc.) and/or using observations by remote sensing instruments, like global positioning system (GPS) ground-receivers or microwave radiometers (MWRs). These instruments allow almost continuous monitoring (with a sampling rate ranging from a few seconds to a few minutes) of atmospheric parameters, such as water vapor content, which is critical for an accurate meteorological forecast. Among GPS data, integrated precipitable water vapor (IPWV) and zenith total delay (ZTD) are used to validate weather prediction model results.

Recently, a few studies on IPWV using both numerical prediction models and GPS data have been carried out with the intent of validating both models and observations. IPWV from the fifth-generation Mesoscale Model (MM5) [1] has been compared with observations from GPS, microwave radiometers, and very long baseline interferometry (VLBI) for three European stations [2]; sparse radiosonde observations (RAOBs) were also used in this study. The authors found a correlation coefficient ranging between 0.75–0.95 and an error bias between MM5 and GPS ranging from 0.0–0.6 cm. Another study found an error bias of approximately 0.3 cm between the MM5 IPWV and GPS IPWV for a few selected stations [3]. Finally, the GPS and the MM5 ZTD have been compared for a mesoscale convective system in the Mediterranean region [4]. The authors found an increasing error during the maximum activity of the convective system.

In this paper, a comparison between IPWV observations collected for about one year at five different sites (Cagliari, Elba Island, Matera, Perugia, and Pomezia) and the output of the MM5 forecast, used as independent estimator of IPWV, is presented. The purpose of this study is to contribute to the understanding of the daily and seasonal variability of the IPWV. The variability associated with the location of the different measurements is also addressed. This analysis would also give an estimation of the error associated with using the model output as a first approximation of climatological data in those locations where instruments are not present, or in testing instrument performances where other measurements are not available. The instruments and the model characteristics are presented in Section II. The instrument comparison is presented in Section III. The IPWV variability is discussed in Section IV, and the conclusions are given in Section V.

Manuscript received May 14, 2004; revised November 17, 2004.

A. Memmo, T. Paolucci, and D. Cimini are with the Center of Excellence (CETEMPS), University of L'Aquila, 67010 Coppito (AQ), Italy (e-mail: Adelaide.memmo@aquila.infn.it; Tiziana.paolucci@aquila.infn.it; nico.cimini@aquila.infn.it).

E. Fionda is with the Ugo Bordoni Foundation, 00142 Rome, Italy (e-mail: ermanno@fub.it).

R. Ferretti is with the Department of Physics and also with the Center of Excellence (CETEMPS), University of L'Aquila, 67010 Coppito (AQ), Italy (e-mail: rossella.ferretti@aquila.infn.it).

S. Bonafoni is with the Department of Electric and Informatics Engineering, University of Perugia, 06125 Perugia, Italy (e-mail: bonafoni@diei.unipg.it).

P. Ciotti is with the Department of Electric Engineering and also with the Center of Excellence (CETEMPS), University of L'Aquila, 67040 Poggio di Roio (AQ), Italy (e-mail: p.ciotti@ing.univaq.it).

Digital Object Identifier 10.1109/TGRS.2004.841488

TABLE I  
FEATURES OF GROUND-BASED MICROWAVE RADIOMETER MWR1 AND MWR2

Specifications	MWR1	MWR2
Operating frequencies	23.80, 31.65 GHz	23.80, 31.40 GHz
Integration time ( $\Delta T$ )	1, 2, 4, 8, 16, 32 sec.	30 – 60 sec.
Radiometric resolution	0.3 K at $\Delta T=1$ sec.	0.25 K
Radiometric accuracy	1 K	0.3 K
Dual-side bandwidth	40 MHz	400 MHz
3-dB antenna beamwidth	1.9° at 23.80 GHz	5.7° at 23.8 GHz
	1.8° at 31.65 GHz	4.4° at 31.4 GHz
Viewing angle	All sky	All sky
Dimensions	150x65x100 cm	50x28x76 cm
Weight	200 kg	21 kg

## II. INSTRUMENTAL AND MODEL DATA

### A. Ground-Based Microwave Radiometers

The Fondazione Ugo Bordoni (FUB) has an experimental station in Pomezia, Italy. This site is placed in a country area south of Rome, between the city and the Tyrrhenian Sea, about 4 km from the coast. A ground-based microwave radiometer (MWR1) is operating in the FUB experimental station. The MWR1 radiometer is a dual-channel system at 23.8 and 31.65 GHz, manufactured by RESCOM Company, Aalborg, Denmark). The main technical characteristics of the MWR1 are summarized in Table I. The MWR1 consists of offset-feed antenna parabolic reflectors connected to microwave receivers of the noise balancing type. Heated air is blown across the antenna reflector to prevent formation of dew and the accumulation of precipitation. Moreover, air from a heater box is directed through a tube to the feed horn window. In this way, the window is kept free from condensation or rain drops.

During the Environmental Satellite (ENVISAT) validation campaign, a portable dual-channel radiometer (MWR2) has been used in a site at Elba Island, in the Tyrrhenian Sea. The MWR2 radiometer is a ground-based sensor manufactured by the Radiometrics Corporation, Boulder, CO. As the MWR1, MWR2 is managed by FUB. The main technical features are reported in Table I. The MWR2 operates at 23.8 and 31.4 GHz. It has been designed to work continuously in unattended mode in almost all weather conditions and for easy portability. An elevation mirror controlled by a step-motor allows the observation of selected sky locations that reflect radiation on the antenna system. The antenna consists of a 15-cm aperture optical Gaussian lens that focuses into a corrugated feed horn. Special baffles and absorbing collars are utilized to minimize errors due to sidelobes and reflections. A blower system prevents the formation of dew and the accumulation of light drizzles upon the antenna radome, but is inefficient for rain events. Regular calibration is provided by tipping-curve method [5].

The IPWV is estimated using a dual-channel ground-based radiometer, with one frequency mainly sensitive to water vapor (subscript 1) and the other to the liquid (subscript 2), at the zenith in a nonscattering atmosphere in local thermodynamic equilibrium [6]. Therefore, IPWV can be expressed as

$$\text{IPWV} = a_0 + a_1\tau_1 + a_2\tau_2 \quad (1)$$

where  $\tau_1$  and  $\tau_2$  (in nepers) are the total atmospheric opacities (at both frequencies) derived from the measured radiometric

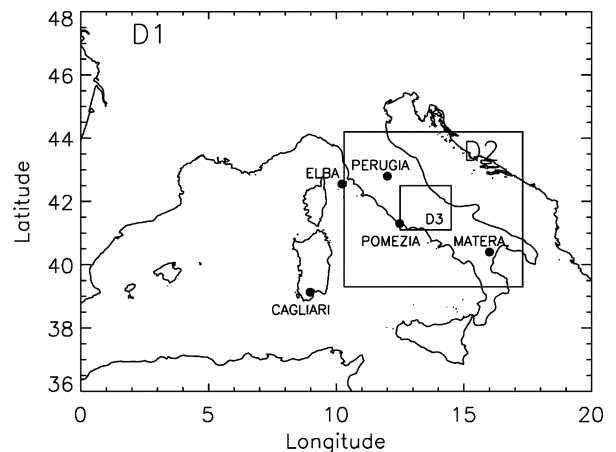


Fig. 1. MM5 model domains and instruments locations. (D1) Coarse domain. (D2) First nested domain. (D3) Innermost domain.

brightness temperatures (in kelvin). Moreover,  $a_0$ ,  $a_1$ , and  $a_2$  are statistical retrieval coefficients, summarizing the microwave properties of the atmosphere [7], [8].

### B. GPS Ground-Based Receivers

In this paper, the data derived from the permanent Italian Fiducial GPS network, managed by Italian Space Agency (ASI), are also used. The national network includes about 20 ground-receivers integrated in the large European GPS Network (EUREF) and in the International GPS Service from Geodynamic applications (IGS) GPS networks. All the data from the Italian Fiducial GPS network are processed using the GIPSY-OASIS II software package [9] with the Precise Point Positioning [10] mode; the sampling rate is equal to 5 min.

The time-varying atmospheric neutral ZTD is retrieved from GPS data. ZTD is the excess path length due to the signal travel (expressed in, for example, centimeters), and it is defined as [11]

$$\text{ZTD} = \text{ZHD} + \text{ZWD} \quad (2)$$

where ZHD is the zenith hydrostatic delay, and ZWD is the zenith wet delay. If the surface pressure is known, ZHD is computed using a simple model [12], whereas ZWD is computed by subtracting ZHD from ZTD. The surface pressure was recorded by precise barometers colocated with GPS receivers during the observing period. Finally, IPWV (centimeters) is estimated from GPS using the following relationship [11]:

$$\text{IPWV} = \pi * \text{ZWD} \quad (3)$$

where  $\pi$  is a nearly constant ( $\pi^{-1} \sim 6.5$ ) function of several physical parameters and of the weighted mean temperature of the atmospheric water vapor. In this study, the monthly averaged values of  $\pi$  obtained from a historical data base of radiosonde [8] are used.

### C. Radiosonde

The radiosonde observations represent the conventional *in situ* measurements. RS-80 Vaisala radiosondes are launched by Italian Air Force Services four times a day (at 00, 06, 12, and 18 UTC) from the Cagliari-Elmas Airport and from the Pratica di Mare station. The former site is located at approximately

TABLE II  
INSTRUMENTS AND OBSERVATION PERIODS FOR EACH STATION

Station	Geographic location		Domain	Observation	Instrument
	Latitude	Longitude			
Perugia	43.1194°	12.3557°	D2	Aug 2002 - Sep 2003	GPS
Elba Island	42.7547°	10.2185°	D1	Aug - Dec 2002	GPS, MWR2
Pomezia	41.6833°	12.4833°	D2	Aug 2002 - Dec 2003	MWR1, RAOBs
Matera	40.6491°	16.7945°	D2	Aug 2002 - Apr 2003	GPS
Cagliari	39.1359°	10.2183°	D1	Apr.- Sep. 2003 Jan.- Dec 2003	GPS, RAOBs

15 km away from the GPS site, and the second one at about 2 km from the radiometric experimental station in Pomezia.

The radiosonde data provide the water vapor distribution with high vertical resolution. However, RAOBs suffer from poor temporal resolution and insufficient spatial sampling. As a consequence, rapid temporal variations of water vapor cannot be monitored.

A good approximation of IPWV can be obtained by integrating directly the measured water vapor profile. The comparison between IPWV derived from different sensors and from RS-80 Vaisala highlighted a few discrepancies [13], [14]. These studies revealed that the Vaisala RS-80 humidity sensor is affected by a dry-bias problem due to contamination by its packaging, and thus a correction to the measured humidity value is usually beneficial [15]. As explained in [13] and [15], the correction is based on the age of the radiosonde (i.e., interval between calibration time and launch time). As an example, the Vaisala's algorithm gives a correction of about 6% for a six-month old radiosonde [14].

Unfortunately, the radiosonde identification number, which express the age, was not available to the authors and thus no correction has been applied in this paper to the RS-80 humidity measurements.

#### D. Numerical Weather Prediction Model

The daily operational forecast carried out at CETEMPS (University of L'Aquila) is used for this study. The forecast is performed using MM5 [1], [16], [17], which is a nonhydrostatic, primitive-equation model with sigma terrain-following vertical coordinates. The sigma coordinate is a function of the pressure ( $p$ ), the surface pressure ( $p_s$ ), and the pressure at the top model level ( $p_t$ )

$$\sigma = \frac{p - p_t}{p_s - p_t}. \quad (4)$$

Sigma varies between 1 at the ground and 0 at the model top (100 hPa). The model has multiple-nesting capabilities to enhance the resolution over the area of interest.

In this study, three two-way nested domains are used, having a grid size of 27, 9, and 3 km (Fig. 1), respectively for domains 1, 2, and 3 (D1, D2, and D3). In addition, 24 unequally spaced  $\sigma$  vertical levels, having a finer resolution at the low levels and decreasing upward,<sup>1</sup> are used. The lowest model level is approximately at 2 m ( $\sigma = 0.999$ ) and the top at approximately 16 000 m ( $\sigma = 0$ ). The model configuration for the forecast

<sup>1</sup>Model sigma levels: 0.999, 0.993, 0.985, 0.975, 0.95, 0.9, 0.85, 0.8, 0.75, 0.7, 0.65, 0.6, 0.55, 0.5, 0.45, 0.4, 0.35, 0.3, 0.25, 0.2, 0.15, 0.1, 0.05, and 0.0.

is the following: the planetary boundary layer parameterization [18], [19] is based on a counter gradient term; the surface energy fluxes are computed following Benjamin [20]; the cumulus convection parameterization [21] is associated with an explicit computation of cloud water and rain for domain 1 and 2, whereas only the explicit computation is used for domain 3. The model is initialized using ECMWF analyses and forecast respectively for the initial and boundary conditions. The operational forecast starts at 1200 UTC every day and lasts for 72 h. For this study, only the hourly model outputs between the 0000 and 2300 UTC of the following day are used. None of the measurements obtained by the instruments are directly employed for the MM5 forecast. Among instrumental data only the radiosondes are used for computing ECMWF analyses, but the model outputs used for this study are extracted in a range of hours (0000–2300 UTC) far away (in time) from the model start time (1200 UTC of the previous day).

### III. INSTRUMENTAL DATA ANALYSIS

The analysis for the different instruments performance is carried out by using data from three different sites (Fig. 1): Cagliari, Elba Island, and Pomezia. This allows for a comparison of the different instruments at the same location. A summary of all the instruments available for each station, and the length of the measurement record is reported in Table II.

#### A. Cagliari Station

At the Cagliari station, the data from GPS and RAOBs were recorded. It should be noticed that radiosondes are available for the entire year 2003, whereas GPS measurements were collected during two seasons only: spring and summer. The IPWV scatter plot for GPS and RAOBs shows a slight underestimation of IPWV by RAOBs with respect to the one by GPS (Fig. 2), for the spring and summer seasons. A bias of  $-0.102$  cm is consistent with the expected value for the RS-80 sensor [14]. A relatively small standard deviation (std) of 0.242 cm and high correlation coefficient (cc) of 0.925 suggest an overall good agreement between GPS and RAOBS (Table III).

#### B. Elba Island Station

The data collected by MWR2 and GPS during the ENVISAT Medium Resolution Imaging Spectrometer (MERIS) validation campaign [22] for the site of Elba Island are used. The two instruments were located in different areas separated by about 2.5 km. The radiometer and the GPS receiver were respectively installed at 10 and 230 m a.s.l. Thus, estimates of IPWV from GPS observations had to be scaled of a factor of 14.7% in order

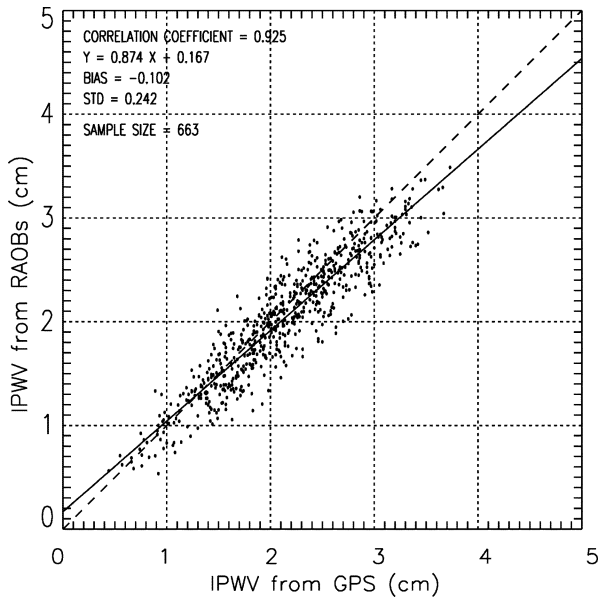


Fig. 2. Scatter plots of IPWV computed at Cagliari from RAOBs versus IPWV from GPS. The solid line represents the linear best fitting.

TABLE III  
STATISTICAL PARAMETERS OF THE IPWV COMPARISONS FOR INSTRUMENTS

Station	Instruments	Bias(cm)	Std(cm)	Corr. Coeff.	Samples
Cagliari	RAOBs – GPS	-0.102	0.242	0.925	663
Elba	GPS – MWR2	-0.001	0.130	0.986	1831
Pomezia	RAOBs – MWR1	-0.118	0.302	0.945	1573

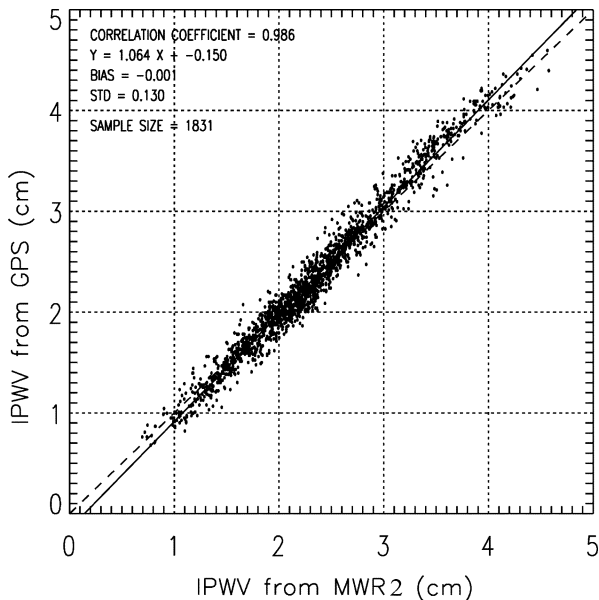


Fig. 3. Scatter plots of IPWV computed at Elba Island from GPS versus IPWV from MWR2. The solid line represents the linear best fitting.

to account for the vertical gap. A climatological dataset for sites close to the sea has been used to estimate the added term. The estimated error was found to be of approximately 3%.

The scatter plot (Fig. 3) shows good agreement between GPS and MWR2, which is also confirmed by the statistical parameters (Table III). A bias of only  $-0.001$  cm, a standard deviation of  $0.13$  cm, and a correlation coefficient of  $0.986$  are found.

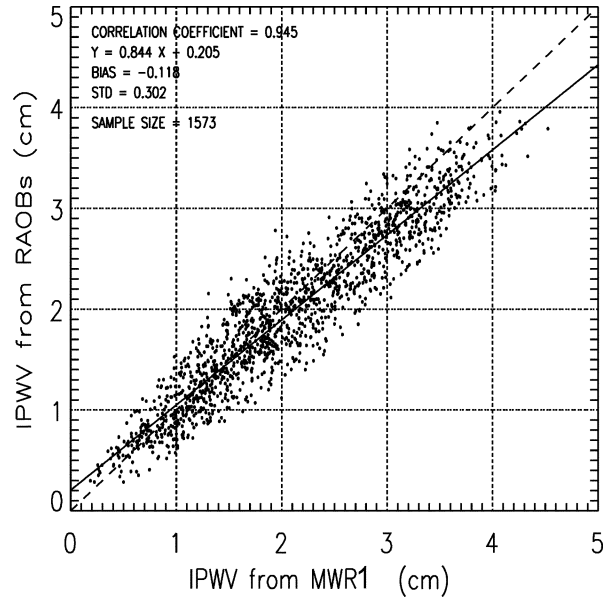


Fig. 4. Scatter plots of IPWV computed at Pomezia from MWR1 versus IPWV from RAOBs. The solid line represents the linear best fitting.

### C. Pomezia Station

At Pomezia station, observations from MWR1 and RAOBs were available. The scatter plot shows (Fig. 4) an underestimation of IPWV by RAOBs with respect to MWR1. The bias of  $-0.118$  cm supports this finding. A standard deviation of  $0.302$  cm and a correlation coefficient of  $0.945$  (Table III) confirm the dry bias of the RAOBs.

## IV. DAILY AND SEASONAL DATA ANALYSIS

The comparison between model forecast and observations is performed to better understand the daily and seasonal variability of IPWV. To this purpose, the same set of data is first analyzed independently on instrument location and is then analyzed considering separately sea and inland sites.

The mean value of IPWV and the anomaly for MWR, GPS, and MM5 are computed for the period August 2002–July 2003, to highlight the daily variability.

The gridded model data are interpolated at station location using a mean weighted distance method for the five grid points surrounding each station. A rough correction is applied to account for the difference between the station altitude and the model topography.

The hourly mean value of IPWV is computed as

$$\overline{\text{IPWV}}_H = \frac{\sum_{n=0,N} \text{IPWV}_n}{N} \quad (5)$$

where  $\text{IPWV}_n$  is either the hourly instrument value or hourly MM5 output (at the hour  $H$ );  $N$  is the total number of observations analyzed. If the hourly mean value of IPWV is computed for the instruments and more than one instrument is available, then all the observations for each instruments are accounted.

The anomaly  $A_H$  for any observation at each hour  $H$  is computed as follows:

$$A_H = \text{IPWV}_H - \overline{\text{IPWV}}_D \quad (6)$$

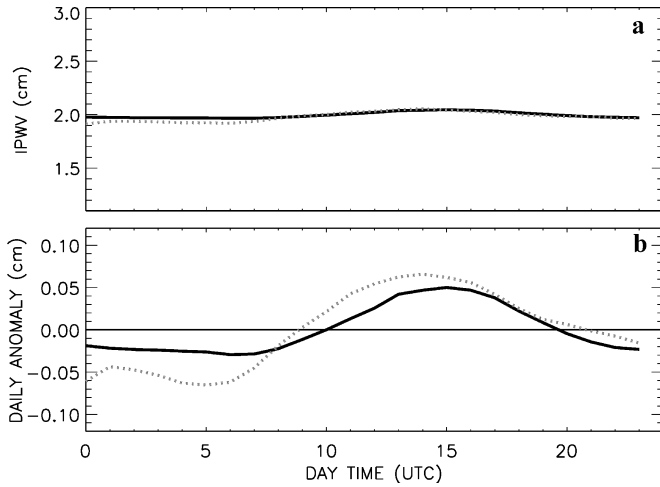


Fig. 5. (a) One-year hourly mean value of IPWV by (bold line) MM5 and (GPS&MWR, dotted line) instruments in top panel. (b) One-year hourly mean daily anomaly (bold line) MM5 and (GPS&MWR, dotted line) instruments in bottom panel.

TABLE IV  
STATISTICAL PARAMETERS OF THE IPWV FOR ONE-YEAR  
COMPARISONS BETWEEN MM5 AND GPS&MWR

Stations	Bias(cm)	Std(cm)	Corr. Coeff.	Samples
All sites	0.001	0.286	0.939	25335
Inland sites	0.022	0.239	0.954	9945
Sea sites	-0.013	0.312	0.923	15390

where  $\overline{IPWV_D}$

$$\overline{IPWV_D} = \frac{\sum_{H=0,23} IPWV_H}{24} \quad (7)$$

is the daily mean value.

#### A. One-Year Daily Analysis

The diurnal IPWV content of the atmosphere, measured by GPS and MWR for all the available sites, shows small variations; only a slight increase during the central hours of the day is found [Fig. 5(a), dotted line]. The MM5 IPWV is in good agreement [Fig. 5(a), solid bold line] with the observations, showing small discrepancies (slightly less than 1 mm) during the first hours of the day (from 0000–0600 UTC). The statistical parameters confirm this agreement: a very small annual bias of 0.001 cm, a high correlation coefficient of 0.939, and a std of 0.286 cm are found (Table IV).

The amplitude of the observed IPWV daily anomaly is likely to be correlated to the surface evapotranspiration processes. In fact, the peak observed in the early afternoon (1400 UTC), and the minimum observed in the early morning (0500 UTC) are strongly related to the maximum evaporation and condensation processes driven by the surface temperature [Fig. 5(b)]. The observed maximum amplitude of the anomaly is 0.7 mm for the instruments. A similar diurnal cycle was found in [23] during the summer in the central U.S. for several GPS receivers. The maximum positive anomaly during the central part of the day is underestimated by the model forecast (0.5 mm). Similarly, the minimum value of the observed IPWV in the early morning

is not well reproduced by the model; indeed the MM5 negative anomaly is smaller than the observed one. The discrepancies between MM5 IPWV and the observed one may be related to the ability of the model to correctly reproduce the diurnal temperature cycle. During the Mesoscale Alpine Programme (MAP) campaign, MM5 showed shortcomings in reproducing the temperature diurnal cycle [24].

#### B. Inland and Sea Sites Data Analysis

To better address the diurnal variability of IPWV, the following analysis is performed separating the sea-side sites (Cagliari, Pomezia and Elba) from the inland ones (Perugia and Matera). This allows the separation of different physical processes producing the water vapor content variability such as convection, advection, evapotranspiration, etc. Indeed, the separation into sea and inland sites allows for enhancing the diurnal variability independently on the background water vapor content which is higher for the sea sites and lower for the inland ones [Fig. 6(a) and (b), respectively, dotted line]. The anomaly clearly shows a larger diurnal variability for the sea sites than for the inland ones. This maximum positive anomaly is mostly driven by the summer season variability at both sites, as the analysis of the diurnal variability for the summer season suggests. The high temperature (summer) allows for developing either transport processes (sea-breeze) on the sea sites and moist-convective processes inland, producing an enhanced IPWV content cycle during summer. The comparison between the amplitude of the anomaly on the two sites clearly shows a reduced variability for the inland with respect to the sea sites. This may be related to the overall lower temperature at the inland sites than at the sea ones. The model clearly reproduces the different mean IPWV for the two sites, higher at the sea than at the inland ones [Fig. 6(a) and (b), respectively, bold solid line], but it fails in reproducing the diurnal variability. In Table IV, the statistical parameters clearly show a model bias larger at the inland sites than at the sea ones (respectively 0.022 and -0.013 cm). On the contrary, a larger variability is found at the sea site than at the inland ones (respectively std = 0.312 cm, cc = 0.923 and std = 0.239 cm, cc = 0.954). A large underestimation of the positive anomaly is found for the sea sites associated to a time delay [Fig. 6(c)], whereas an overestimation of the minimum is found at both sites [Fig. 6(c) and (d)]. The model forecast clearly shows difficulties in reproducing the large sea site variability.

#### C. Seasonal Data Analysis

The spatial variability of the water vapor content of the atmosphere has been also studied in [25] for the GPS only. The authors analyzed the spatial variability of the water vapor content in terms of ZWD; they found a larger variability of water vapor content during the summer than during the winter.

The seasonal analysis of the IPWV produced by GPS and MWR is performed to better understand its diurnal cycle and its relationship with the temperature. Similarly to the daily analysis mean and anomaly are used for the seasonal analysis. The four seasons are divided into: summer (June, July, and August), autumn (September, October, and November), winter (December, January, and February), and spring (March, April,

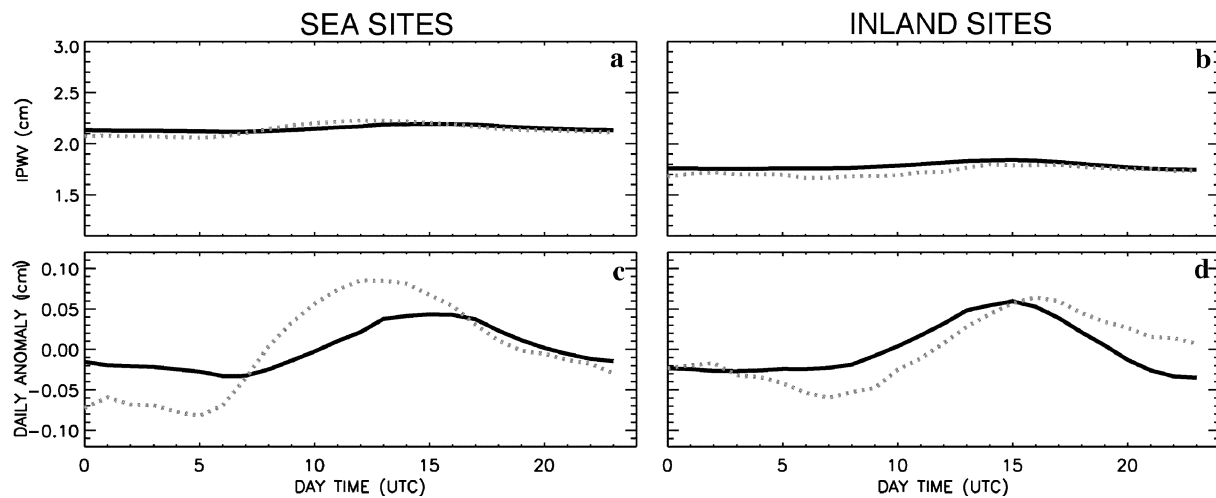


Fig. 6. (a) One-year hourly mean value of IPWV by (bold line) MM5 and (GPS&MWR, dotted line) instruments at sea sites. (b) One-year hourly mean value of IPWV by (bold line) MM5 and (GPS&MWR, dotted line) instruments at inland sites. (c) One-year hourly mean daily anomaly (bold line) MM5 and (GPS&MWR, dotted line) instruments at sea sites. (d) One-year hourly mean daily anomaly (bold line) MM5 and (GPS&MWR, dotted line) instruments at inland sites.

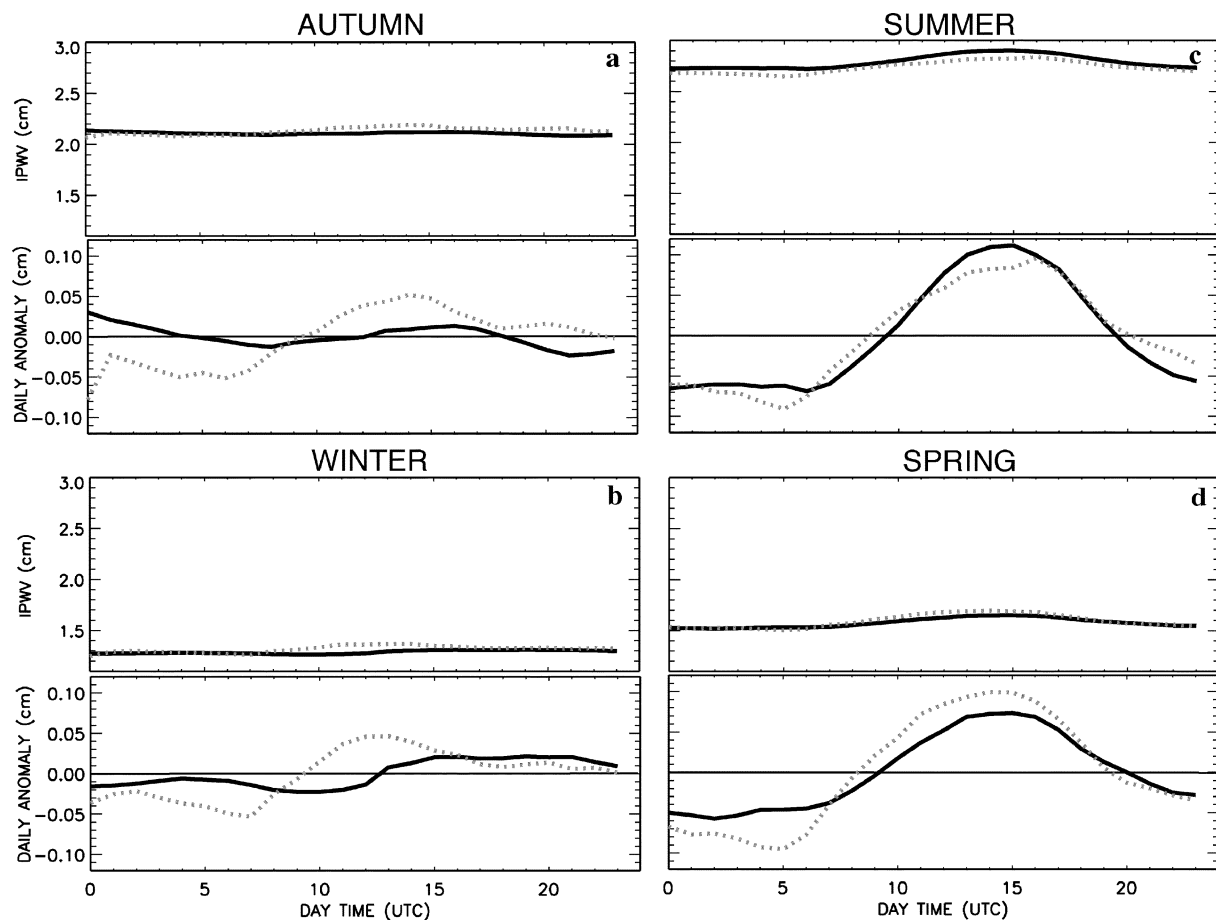


Fig. 7. (a) Autumn hourly mean value of IPWV by (bold line) MM5 and (GPS&MWR, dotted line) instruments in top panel. Autumn hourly mean daily anomaly (bold line) MM5 and (GPS&MWR, dotted line) instruments in bottom panel. (b) Winter hourly mean value of IPWV by (bold line) MM5 and (GPS&MWR, dotted line) instruments in top panel. Winter hourly mean daily anomaly (bold line) MM5 and (GPS&MWR, dotted line) instruments in bottom panel. (c) Summer hourly mean value of IPWV by (bold line) MM5 and (GPS&MWR, dotted line) instruments in top panel. Summer hourly mean daily anomaly (bold line) MM5 and (GPS&MWR, dotted line) instruments in bottom panel. (d) Spring hourly mean value of IPWV by (bold line) MM5 and (GPS&MWR, dotted line) instruments in top panel. Spring hourly mean daily anomaly (bold line) MM5 and (GPS&MWR, dotted line) instruments in bottom panel.

and May). The IPWV diurnal cycle clearly appears (Fig. 7) during the strong solar forcing periods (summer and spring), whereas is much smaller during the other seasons (winter and autumns), for both instruments and MM5. Also, in this case, the

reduced IPWV variability is related to the low temperature of the cold season as for the inland sites: during the winter season the atmosphere is cold and more advective than in summer, reducing the amplitude of the anomaly of IPWV. The seasonal

TABLE V  
STATISTICAL PARAMETERS OF THE IPWV FOR SEASONAL  
COMPARISONS BETWEEN MM5 AND GPS&MWR

Stations	Bias(cm)	Std(cm)	Corr. Coeff.	Samples
Autumn	-0.029	0.286	0.909	7963
Winter	-0.011	0.185	0.934	5612
Spring	-0.007	0.248	0.921	5534
Summer	0.068	0.389	0.768	6226

TABLE VI  
STATISTICAL PARAMETERS OF THE IPWV COMPARISONS  
BETWEEN MM5 AND RAOBS

Period	Bias(cm)	Std(cm)	Corr. Coeff.	Samples
1 Year	0.054	0.315	0.924	1572
Autumn	-0.082	0.307	0.883	180
Winter	-0.018	0.186	0.929	338
Spring	0.065	0.257	0.908	602
Summer	0.164	0.426	0.713	452

analysis clearly highlights the variation of the observed total amount of IPWV hourly mean reaching a maximum of 2.9 cm [Fig. 7(c), top panel] during the summer and a minimum of 1.2 cm [Fig. 7(b), top panel] during the winter. Small differences are found between MM5 and observed IPWV [Fig. 7(a)–(d) in the top panel, respectively bold and dotted lines] Generally, MM5 slightly underestimates IPWV (less than 1 mm), except during the summer where a maximum overestimation of 1 mm is found [Fig. 7(c), top panel]. This would produce a mean seasonal MM5 error of approximately 3% during the summer and 8% during the winter. This is confirmed by the statistical parameters, which show an underestimation for all seasons except for summer (Table V). A maximum spread associated with a minimum correlation is also found for summer (Table V).

The observed IPWV diurnal anomaly clearly shows remarkable differences among the seasons [Fig. 7(a)–(d) in bottom panel, dotted lines]: large values of the anomaly, either positive or negative, are found only during the warm seasons (summer and spring). In summer, the amplitude of the diurnal variation is approximately 1 mm, in good agreement with what found in [23] during the same season in the U.S., for the GPS ground receivers. The large variation, recorded during summer, is gradually reduced during the other seasons reaching the minimum amplitude in autumn and winter. Generally, the MM5 IPWV forecast is in good agreement with the observations, largely reproducing the diurnal cycle for the seasons [Fig. 7(c) and (d), bottom panel] having a strong solar forcing, but also an overestimation is found during the summer. The maximum observed amplitude at noon (1000–1500 UTC) is overestimated by MM5, whereas an underestimation and a time delay (1 h) is found for the minimum [Fig. 7(c), bottom panel]. The underestimation of the minimum of the diurnal amplitude is relatively larger during the other seasons than during summer. Moreover, during the cold seasons, the MM5 forecast [Fig. 7(a) and (b)] smoothes out most of the diurnal cycle, and it is out of phase with respect to the observations. These discrepancies between the forecast and the observations may be related to the already pointed out MM5 shortcoming in forecasting the temperature diurnal cycle

[24] and to a limiting factor produced by the parameterization of the soil moisture availability, which does not follow a diurnal cycle. This discrepancy is enhanced during the cold season because the prevailing advective processes tend to overwhelm the diurnal cycle producing a weak signal difficult to forecast.

#### D. RAOBs Versus MM5

Finally, an annual and seasonal analysis is performed separately using IPWV from RAOBs and MM5. It was necessary to separate RAOBs from the other instruments because their sampling rate is limited to only four daily observations. The agreement between MM5 and RAOBs is poorer than the one found between MM5 and the other instruments: a larger bias (0.054 cm) associated with a larger std (0.315 cm) and a lower cc (0.924) are found (Table VI). The seasonal analysis confirms the annual trend showing an overall larger bias (maximum during the summer 0.164 cm), std (maximum during the summer 0.426 cm), and a minimum cc (during the summer 0.713), with respect to the other instruments (Table VI) The discrepancies found between RAOBs and MM5 is likely produced by the dry bias of the VAISALA-RS80 radiosonde, as previously pointed out. This hypothesis is supported by the disagreement found also between RAOBs and the other instruments. The increased error during the summer may be produced by the sensor arm heating error, which is largely correlated to the increase of the temperature [15].

#### V. CONCLUSION

The results presented in this study show a good agreement among the IPWV measured by different instruments (RAOBs, GPS, and MWRs), and a fairly good agreement between observations and the forecast of IPWV.

Both the scatter plots and the statistical parameters show a very good agreement between the GPS and MWR data, whereas a slightly poorer agreement is found between RAOBs and the other instruments. This is likely produced by the dry bias of RAOBs.

The comparison among statistical parameters (bias, standard deviation, and correlation coefficient) for the different seasons highlights an increase of the MM5 error during the warm months. Indeed, the correlation coefficient is smaller for summer than for the other seasons; it is also smaller than the annual value. Bias and std also suggest an IPWV overestimation by MM5, but both these statistical parameters are related to the total amount of water vapor content of the atmosphere, in particular a larger amount of IPWV produces a larger bias. Because of the larger IPWV content during the summer than during the other season, also a greater bias is expected. The instruments also highlighted the spatial variability of the water vapor content.

The analysis of the amplitude of the diurnal cycle, for both annual and seasonal data, highlights the IPWV diurnal cycle dependence from both the location and the season. Moreover, it was found an MM5 shortcoming in forecasting IPWV, which is related to the well-known difficulties in reproducing the temperature diurnal cycle. During the early morning, the overestimation of water vapor content in the lower layer of the troposphere produces (or it is produced by) the warm temperature

bias. The relationship between the MM5 temperature and water vapor content bias has to be further investigated, as is the soil moisture availability in the evapo-transpiration processes.

#### ACKNOWLEDGMENT

The authors wish to thank R. Pacione (Telespazio SPA, Rome, Italy) and F. Vespe (Agenzia Spaziale Italiana, Matera, Italy) for the computation regarding GPS data. The authors thank the anonymous reviewers for their suggestions that largely improved the paper.

#### REFERENCES

- [1] G. A. Grell, J. Dudhia, and D. R. Stauffer, "A description of fifth-generation Penn State/NCAR mesoscale model (MM5)," Nat. Center Atmos. Res., Boulder, CA, NCAR Tech. Note NCAR/TN-398+STR, 1994.
- [2] D. Behrend, R. Haas, L. P. Gradinarsky, S. J. Keihm, W. Schwarz, L. Cuccurull, and A. Rius, "MM5 derived ZWD's compared to observational results from VLBI, GPS and WVR," *Phys. Chem. Earth*, vol. 27, pp. 301–308, 2002.
- [3] R. Pacione, C. Sciarretta, F. Vespe, C. Faccani, R. Ferretti, E. Fionda, C. Ferraro, and A. Nardi, "GPS meteorology, validation and comparisons with ground-based microwave radiometer and mesoscale model for the Italian GPS permanent stations," *Phys. Chem. Earth, Part Solid Earth Geodesy*, vol. 26, pp. 139–145, 2001.
- [4] L. Cuccurull, J. Vila, and A. Rius, "Zenith total delay study of mesoscale convective system: GPS observations and fine-scale modeling," *Tellus Series A—Dinamic Meteorol. Oceanogr.*, vol. 54, pp. 138–147, 2002.
- [5] Y. Han and E. R. Westwater, "Analysis and improvement of tipping calibration for ground-based microwave radiometers," *IEEE Trans. Geosci. Remote Sens.*, vol. 38, no. 3, pp. 1260–1276, May 2000.
- [6] E. R. Westwater and F. O. Guiraud, "Ground-based microwave radiometric retrieval of precipitable water vapor in the presence of clouds with high liquid content," *Radio Sci.*, vol. 15, pp. 947–957, 1980.
- [7] P. Basili, P. Ciotti, and E. Fionda, "Accuracy of physical, statistical and neural network based algorithms for the retrieval of atmospheric water by ground-based microwave radiometry," in *Proc. IGARSS*, Seattle, WA, July 1998, pp. 418–420.
- [8] P. Basili, S. Bonafoni, R. Ferrara, P. Ciotti, E. Fionda, and R. Ambrosini, "Atmospheric water vapor retrieval by means of both a GPS network and a microwave radiometer during an experimental campaign at Cagliari (Italy) in 1999," *IEEE Trans. Geosci. Remote Sens.*, vol. 39, no. 11, pp. 2436–2443, Nov. 2001.
- [9] F. H. Webb and J. F. Zumberge, *An Introduction to GIPSY/OASIS II*, Jet Propulsion Lab., Pasadena, CA, 1997.
- [10] J. F. Zumberge, M. B. Hefflin, D. C. Jefferson, M. M. Watkins, and F. H. Webb, "Precise point positioning for the efficient and robust analysis of GPS data from large networks," *J. Geophys. Res.*, vol. 102, no. B3, pp. 5005–5017, 1997.
- [11] M. Bevis, S. Businger, S. Chiswell, T. A. Herring, R. A. Anthes, C. Rocken, and R. H. Ware, "GPS meteorology mapping Zenith wet delays onto precipitable water," *J. Appl. Meteorol.*, vol. 33, pp. 379–386, 1994.
- [12] J. Saastamoinen, "Atmospheric correction for the troposphere and stratosphere in radio ranging of satellite," in *The Use of Artificial Satellite for Geodesy*, ser. Geophysics Monographs.. Washington, DC: Amer. Geophy. Union, 1972, vol. 15, pp. 247–251.
- [13] B. M. Lesht, "Reanalysis of radiosonde data from the 1996 and 1997 water vapor intensive observation periods: Application of the Vaisala RS-80H contamination correction algorithm to dual-sonde soundings," in *Proc. 9th ARM Science Team Meeting*, San Antonio, TX, Mar. 22–26, 1999, [Online]. Available: [http://www.arm.gov/docs/documents/technical/conf\\_9903/lesht-99.pdf](http://www.arm.gov/docs/documents/technical/conf_9903/lesht-99.pdf).
- [14] E. R. Westwater, B. B. Stankov, D. Cimini, Y. Han, J. A. Shaw, B. M. Lesht, and C. N. Long, "Radiosonde humidity soundings and microwave radiometers during Nauru99," *J. Atmos. Ocean. Technol.*, vol. 20, no. 7, pp. 953–971, Jul. 2003.
- [15] J. Wang, H. L. Cole, D. J. Carlson, E. R. Miller, K. Beierle, A. Paukkunen, and T. K. Laine, "Corrections of humidity measurement errors from the Vaisala RS80 radiosonde application to TOGA COARE data," *J. Atmos. Oceanic Technol.*, vol. 19, pp. 981–1002, 2002.
- [16] R. Anthes and T. T. Warner, "Development of hydrodynamic models suitable for air pollution and other meteorological studies," *Mon. Weather Rev.*, vol. 106, pp. 1045–1078, 1978.
- [17] J. Dudhia, "A nonhydrostatic version for the Penn-State-NCAR mesoscale model: Validation test and simulation of an Atlantic cyclone and cold front," *Mon. Weather Rev.*, vol. 121, pp. 1493–1513, 1993.
- [18] Y. H. Hong and H. L. Pan, "Non-local boundary layer vertical diffusion in medium range forecast model," *Mon. Weather Rev.*, vol. 124, pp. 2322–2339, 1996.
- [19] I. Troen and L. Marth, "A simple model of atmospheric boundary layer: Sensivity to surface evaporation," *Bound. Layer Meteorol.*, vol. 37, pp. 129–148, 1986.
- [20] S. G. Benjamin, "Some effect of surface heating and topography on the regional severe storm environment," Ph.D. thesis, Dept. Meteorol., Pennsylvania State Univ., University Park, 1983.
- [21] J. S. Kain and J. M. Fritsch, "A one-dimensional entraining/detraining plume model and its application in convective parameterization," *J. Atmos. Sci.*, vol. 47, pp. 2784–2802, 1990.
- [22] P. Ciotti, E. Di Giampaolo, P. Basili, S. Bonafoni, V. Mattioli, R. Biondi, E. Fionda, F. Consalvi, A. Memmo, D. Cimini, R. Pacione, and F. Vespe, "Validation of MERIS water vapour in the central Italy by concurrent measurements of microwave radiometers and GPS receivers," in *Proc. IGARSS*, Toulouse, France, Jul. 21–25, 2003.
- [23] A. Dai, J. Wang, R. H. Ware, and T. Van Hove, "Diurnal variation in water vapor over North America and its implications for sampling errors in radiosonde humidity," *J. Geophys. Res.*, vol. 107, pp. ACL 11-1–ACL 11-14, 2002.
- [24] R. Ferretti, T. Paolucci, G. Giuliani, T. Cherubini, L. Bernardini, and G. Visconti, "Verification of high t-resolution real-time forecast over the Alpine region during the MAP SOP," *Q. J. R. Meteorol. Soc.*, vol. 129, pp. 587–607, 2003.
- [25] B. Stoew and G. Elgered, "Characterization of atmospheric parameters using a ground based GPS network in North Europe," *J. Meteorol. Soc. Jpn.*, vol. 82, pp. 587–596, 2004.

**Adelaide Memmo** was born in Chieti, Italy, in 1971. She received the Laurea degree in Astronomy in 1996 from the University of Bologna, Italy. Between 1997 and 2002 she was with PSTd'A (Scientific and Technologic Park of Abruzzo) in L'Aquila, working with a five channel microwave radiometer and then with MM5 model (Mesoscale Model 5) developed by Pennsylvania State University and National Center for Atmospheric Research (PSU/NCAR), dealing particularly with observation nudging technique. During 2002 she collaborated with the Italian Space Agency (ASI) in the MAGIC project for the validation of GPS data; she also collaborated with Center of Excellence (CETEMPS) for the ground validation of ENVISAT data. Since november 2002, she is working with CETEMPS to supply a meteorological support to the ASI base of Trapani for the forecast of stratospheric balloon trajectories. She is also working on the empirical validation of MM5 model data.

**Ermanno Fionda** received the laurea degree in physics from the University of Roma "La Sapienza," Rome, Italy, in 1980, and the Ph.D. degree in electronic and information engineering from the University of Perugia, Perugia, Italy, in 2003.

From 1981 to 1982 he was with the Atmospheric Physics Institute (IFA-CNR, Roma) where he worked on the energetic balance in the lower atmospheric layer. Since 1983, he has been with the "Ugo Bordoni" Foundation, Rome. His major research experience has been on various influences of the earth's atmosphere on radio waves for communication, as well as remote sensing techniques. His particular areas of interest are scintillation, scattering and absorption-emission processes using satellite links and ground-based microwave radiometers. He has been a Visiting Fellow with the National Oceanic and Atmospheric Administration's Environmental Technology Laboratory/Wave Propagation Laboratory, Boulder, CO. He is currently involved in the studies of water vapor estimation using ground and airborne sensors in the framework of the validation campaign ENVISAT managed by the European Space Agency.



**Tiziana Paolucci** was born in 1964. She received the laurea degree in physics in 1992 from the University of L'Aquila, L'Aquila, Italy.

Since 1992, she has been working on the MM5 Model (Mesoscale Model 5). She has collaborated with the University of L'Aquila to realized an operational MM5 real-time forecast. She is also participating in the MAP campaign with the MM5 operational in the northern Italian Alps and the APEGAlA campaign. She has collaborated with the Atmospheric Modeling WP, Center of Excellence CETEMPS, University of L'Aquila, on the high-resolution weather forecast. She is currently working with the Regional Meteorological Service.



**Domenico Cimini** (M'03) was born in Teramo, Italy, in 1973. He received the laurea (cum laude) and Ph.D. degrees from the University of L'Aquila, L'Aquila, Italy, in 1998 and 2002, respectively, both in physics.

He has collaborated with the Environmental Technology Laboratory (ETL), National Oceanic and Atmospheric Administration (NOAA), Boulder, CO since 1999. From 2000 to 2004, he participated in two Water Vapor Intensive Operational Periods, held at the Atmospheric Radiation Measurement program's Southern Great Plain and North Slope of

Alaska sites. Since 2002, he has been with the Center of Excellence CETEMPS, University of L'Aquila, Italy, working on radiometer calibration techniques, microwave radiative transfer models, and ground- and satellite-based passive microwave and infrared radiometry. He is currently with the Remote Sensing Division, Center of Excellence (CETEMPS), University of L'Aquila, where he is working on ground- and satellite-based passive microwave and infrared radiometry. Since August 2004, he has been a Visiting Fellow with the Cooperative Institute for Research in Environmental Sciences, University of Colorado, Boulder.

**Rossella Ferretti** was born on March 5, 1956. She received the laurea in physics (summa cum laude) from the University of Rome "La Sapienza," Rome, Italy, in 1980, and the Ph.D. degree in geophysics from the School of Geophysical Sciences, Georgia Institute of Technology, Atlanta, in 1986.

In 1989, she was a Researcher with the Department of Physics, University of L'Aquila. In 1997, she was invited to the National Center for Atmospheric Research to conclude the research started the year before. She started working with Dr. Rotunno on the interaction of real flow over an obstacle. In 1998, The Real-Time forecast at the University of L'Aquila became operational. In 1999, she Participated in the MAP campaign: MM5 operational on the northern Italian Alps and participated in the APEGAlA campaign: MM5 operational in the Terra Del Fuoco and Antarctica. In 2001, she was responsible for the WP "Meteorological Integrated Modeling" for the Centro di Eccellenza "Integration of Remote sensing technique in to numerical model for the heavy precipitation forecast" funded by the MURST. She has been a reviewer for the *Journal of Climate*, *Journal of Atmospheric Science*, *Quarterly Journal of Royal Meteorological Society*, and *Annales Geophysicae*. In 2002, she was responsible for the group of L'Aquila in the UE project TOUGH for the operational assimilation of GPS data. In 2003, she worked in cooperation with CUDAM (Trento): MM5 operational during the campaign in that area. In cooperation with the University of Milano-Bicocca, she worked on the MM5 operational on Rosa Mountain during a campaign on the Lys glacier and MM5 operational with the assimilation of GPS data.



**Stefania Bonafoni** was born in Fabriano, Italy, on March 9, 1971. She received the laurea degree (cum laude) and the Ph.D. degree from the University of Perugia, Perugia, Italy, in 1997 and 2000, respectively, both in electronic engineering.

She is currently a Contract Researcher at the University of Perugia, teaching a course on electromagnetic fields at the IIT, University of Perugia. Her research activity has been concerned with microwave and millimeter-wave propagation in the atmosphere, atmospheric remote sensing by radiometry, and in-

version methods in electromagnetics.



**Piero Ciotti** (M'94) was borne in Rome, Italy, on November 10, 1952. He received the laurea (Doctor) degree (cum laude) in electronic engineering from the University of Rome "La Sapienza," Rome, Italy, in 1977.

He joined the Department of Electronic Engineering, University "La Sapienza," Rome, in 1977, where he served first as an Assistant Professor and, since 1987, as an Associate Professor, teaching a course on remote sensing. Since 1991, he has been with the Department of Electrical Engineering,

University of L'Aquila, L'Aquila, Italy, where he has taught courses on signal theory, electromagnetic fields, and electromagnetic wave propagation. In April 2000, he became a Full Professor of electromagnetics at the same university. During 1984–1985, he conducted research at the Wave Propagation Laboratory, Environmental Research Laboratory, National Oceanic and Atmospheric Administration, Boulder, CO, on a NATO/CNR fellowship. He was a member of the ESA Calibration Team for the ERS-1 Radar Altimeter and a Principal Investigator of the ESA/JRC MAESTRO airborne SAR campaign. He is also Principal Investigator of an ESA/ENVISAT accepted research proposal and member of RA-2/MWR, MERIS, MIPAS, GOMOS, and SCIAMACHY Validation Teams. His research activity has been concerned with microwave remote sensing of the environment, microwave and millimeter-wave atmosphere, microwave line-of-sight propagation, inverse electromagnetic problems, and digital signal processing.